Rubbing-Induced Molecular Reorientation on an Alignment Surface of an Aromatic Polyimide Containing Cyanobiphenyl Side Chains

ARTICLE *in* JOURNAL OF THE AMERICAN CHEMICAL SOCIETY · JULY 2001

Impact Factor: 12.11 · DOI: 10.1021/ja0042682 · Source: PubMed

11 AUTHORS, INCLUDING:

Seok-Cheol Hong
Korea University
52 PUBLICATIONS **889** CITATIONS
SEE PROFILE

yi-ren Shen
China Medical University (ROC)
249 PUBLICATIONS **10,487** CITATIONS
SEE PROFILE

Rubbing-Induced Molecular Reorientation on an Alignment Surface of an Aromatic Polyimide Containing Cyanobiphenyl Side Chains

Jason J. Ge,[†] Christopher Y. Li,[†] Gi Xue,[†,§] Ian K. Mann,[†] Dong Zhang,[†] Shyh-Yeu Wang,[†] Frank W. Harris,[†] Stephen Z. D. Cheng,*[,†] Seok-Cheol Hong,[‡] Xiaowei Zhuang,[‡] and Y. R. Shen[‡]

Contribution from the The Maurice Morton Institute and Department of Polymer Science, The University of Akron, Akron, Ohio 44325-3909, and Department of Physics, University of California Berkeley, Berkeley, California 94720-7300

Received December 15, 2000

Abstract: Surface lamellar decoration (SLD), surface enhanced Raman scattering (SERS) and optical second harmonic generation (SHG) experiments have been utilized to study the molecular orientation and conformation changes at a rubbed polyimide alignment-layer surface. This aromatic polyimide containing pendent cyanobiphenyl mesogens was synthesized via a polycondensation of 2,2′-bis(3,4-dicarboxy-phenyl)hexafluoropropane dianhydride (6FDA) with bis{ω-[4-(4-cyanophenyl)phenoxy]hexyl} 4,4′-diamino-2,2′-biphenyldicarboxylate (*n*CBBP, $n = 6$), abbreviated as 6FDA−6CBBP. Uniform alignment layers, possessing high pretilt angles ranging from 39° to 43°, have been achieved after mechanical rubbing of the polyimide thin film surface at room temperature and subsequent annealing. This is the first time that high pretilt angles have been detected to possess a negative angle ($-\theta_c$) with respect to the rubbing direction (i.e., opposite to the rubbing direction), considerably different from the conventional pretilt angle (θ_c) observed along the rubbing direction. This observation is confirmed using magnetic null and SHG methods. Combined polyethylene (PE) SLD and atomic force microscopy experiments reveal that the azimuthal orientation distribution of the long axis of the edge-on PE lamellar crystals is oriented normal to the rubbing direction, indicating that the PE chains are aligned parallel to the rubbing direction. This SLD technique probes the anisotropic surface orientation of the outermost molecules of the rubbed polyimide layer. The SERS results show that prior to rubbing the surface, both the pendent cyanobiphenyls in the side chains and backbones possess nearly planar chain conformations at the polyimide surface. Mechanical rubbing causes not only tilting of the backbone moieties, such as imide-phenylene structure, but also significant conformational rearrangements of the pendent side chains at the surfaces. The molecular mechanism of this unusual alignment is due to the fact that the pendent cyanobiphenyls forms a uniformly tilted conformation on the rubbed surface, and the polar cyano groups point down toward the layer surface deduced from SHG phase measurements. This conformational rearrangement of the side chains results in the formation of fold-like bent structures on the surface, which directly leads to the long axis of cyanobiphenyls having the $-\theta_c$ pretilt angle with respect to the rubbing direction.

Introduction

High-resolution liquid crystal displays (LCDs), including full color addressed passive matrix super-twisted nematic (STN) LCDs and active matrix thin-film-transistor (TFT) LCDs, are widely used in broadcasting, telecommunications, laptop/desktop computers, and other fields of use.[1] In the mass production of LCDs, polyimide alignment layers play a critical role, via mechanical rubbing, in controlling the bulk orientation of liquid crystals (LC) in a preferential direction. These layers are conventionally spin-coated or rotary-printed on indium tin-oxide glass substrates with a thickness between 50 and 200 nm. It has been speculated that upon mechanical rubbing, the molecular alignment on the layer surface can substantially differ from the bulk. It is important to recognize that high pretilt alignment layers are essential to inhibit the occurrence of the twist nematic (TN) reverse-tilt disclination and the appearance of the STN two-dimensional striped distortion, in addition to reducing the operational voltage.[2] Linearly polarized ultraviolet (UV) photoalignment techniques have also been reported to form anisotropic LC alignment.[3−5]

To achieve a reasonable gray scale for displays, a sufficiently high pretilt angle is required. One of the most significant scientific ideas is whether high pretilt angle alignment layers can be obtained after rubbing by introducing side chains on polyimide backbones for adjusting the structure and chemical properties. Mechanisms of rubbing-induced LC bulk alignment and pretilt angle in LC cells have been actively discussed over the past decade.[6−14] Two major points of view are that first,

* To whom all correspondence should be addressed. E-mail: cheng@polymer.uakron.edu.

[†] The University of Akron.

[‡] University of California Berkeley.

[§] Current address: Department of Macromolecular Science, Nanjing University, Nanjing, China.

(1) Morozumi, S. In *Liquid Crystals*; Bahadur, B., Ed.; World Scientific Publishing: Singapore, 1990; Vol. 1, pp 171−194.

(2) Bos, P. J.; Fredley, D.; Li, J.; Rahman, J. In *Liquid Crystals in Complex Geometries*; Crawford, G. P., Zumer, S., Eds.; Taylor and Francis: Great Britain, 1996; pp. 281−289.

(3) Gibbons, W. M.; Shannon, S. T.; Sun, S. T.; Swetlin, B. J. *Nature* **1991**, *351*, 49−50.

(4) Shannon, P. J.; Gibbons, W. M.; Sun, S. T. *Nature* **1994**, *368*, 532−533.

(5) Schadt, M.; Seiberie, H.; Schuster, A. *Nature* **1996**, *380*, 212−215.

10.1021/ja0042682 CCC: $20.00
Published on Web 05/25/2001

periodic microgrooves (or microtrenches), generated by rubbing, may force the LC molecules at the alignment-layer surface to be parallel to the rubbing direction (topological alignment), due to geometric restrictions between surface microgrooves and LC molecules.[6] Second, van der Waals physical interactions, at the interface between LCs and oriented polymers at alignment-layer surfaces, may play the predominant role in aligning LC molecules.[7] To further explore the molecular mechanism responsible for this surface-induced LC alignment and design new polymer architectures to achieve desirable alignment properties, it requires a deep understanding of the surface chemical and physical structures.

Among the experimental techniques in surface characterization, the optical second harmonic generation (SHG) and sum frequency generation (SFG) vibration spectroscopy are intrinsically surface-sensitive.[8−10] In the second-order nonlinear optical process, it is forbidden in a medium with inversion symmetry, but allowed at surfaces where such symmetry is necessarily broken. Consequently, the polarization dependence of SHG and SFG permits a quantitative determination of surface molecular orientation. Grazing-incidence X-ray scattering experiments have been applied to study the rubbing-induced orientation near the polyimide surface of a semicrystalline polyimide (such as BPDA−PDA), which detects the crystal-orientation profiles along different directions with respect to the rubbing direction.[11] Near-edge X-ray absorption fine structure spectroscopy probes different orientation order parameters of the rubbed polyimide surface (such as PMDA−ODA), deduced from the changes in absorption energies.[12] X-ray photoelectron spectroscopy has probed the surface with binding energy changes at rubbed polymer surfaces in a typical range of 1−5 nm after rubbing.[13,14]

Scanning probe microscopy techniques, such as atomic force microscopy (AFM), have demonstrated surface topologies down to an atomic level in static single crystals.[15,16] However, in almost all the cases of alignment-layer studies, AFM only provides aligned physical scratches on the rubbed surface on a length scale of a few hundred nanometers to micrometers. No individually oriented chain has been clearly observed on a rubbed surface.[17,18] This suggests that we need an effective anisotropic probe to detect chain orientation on the noncrystalline alignment surface when using AFM.

Generally speaking, conventional infrared (IR) and Raman spectroscopy are not surface-sensitive. However, surface-enhanced Raman scattering (SERS) is a unique technique resulting in intense Raman scattering signals from molecules adjacent to a rough silver substrate.[19,20] The enhancement decreases rapidly as a function of distance from the molecular surface, making SERS particularly surface-sensitive. In recent years, SERS techniques have been used to probe single molecular chains and single nanoparticles.[21,22]

Scheme 1. Synthesis of the Side Chain Polyimide Containing Pendent Cyanobiphenyl Mesogens

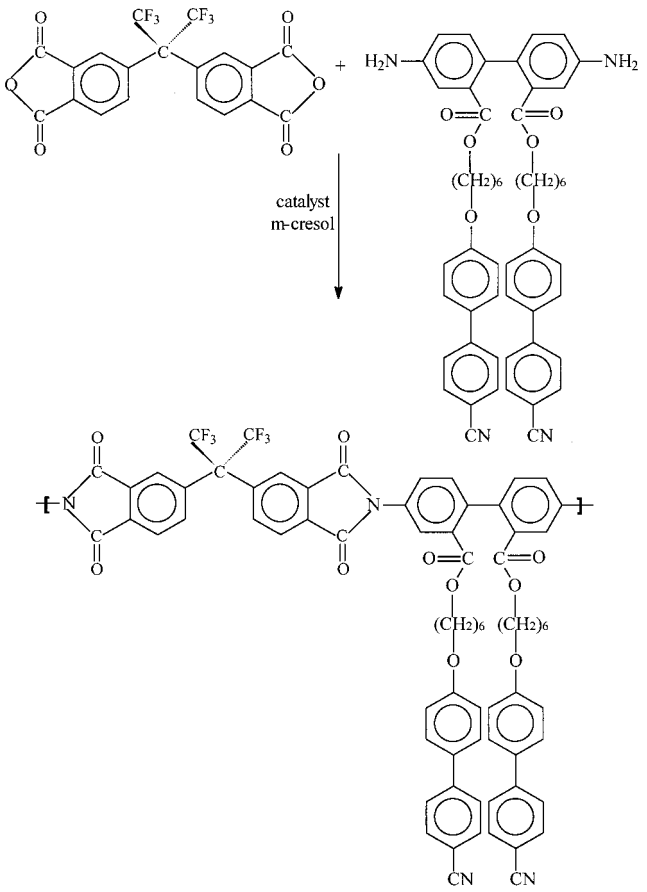

In this study, we focus on a specifically designed aromatic polyimide containing pendent cyanobiphenyl mesogens as an alignment layer having a high pretilt angle. The introduction of cyanobiphenyls in the side chains generates high pretilt angles with a polar interaction to align bulk LC molecules in LCDs. Using several surface-sensitive methods, we report our experimental results on surface chemical and physical structures of this polyimide alignment layer, and provide a new understanding of molecular orientation and conformation changes at the outermost surface after rubbing.

Experimental Section

Materials and Samples. A series of side-chain polyimides containing pendent cyanobiphenyl mesogens was synthesized. One of the polyimides in this series, having six methylene units in the side chains, was chosen for this study (Scheme 1). The key monomer for this polymerization was the new diamine containing pendent cyanobiphenyl mesogens of bis{ω-[4-(4-cyanophenyl)phenoxy]hexyl} 4,4′-diamino-

(6) Berreman, D. W. *Phys. Rev. Lett.* **1972**, *28*, 1683−1686; *Mol. Cryst. Liq. Cryst.* **1973**, *23*, 215−232.
(7) Geary, J. M.; Gooby, J. W.; Kmetz, A. R.; Patel, J. S. *J. Appl. Phys.* **1987**, *62*, 4100−4108.
(8) Feller, M. B.; Chen, W.; Shen, Y. R. *Phys. Rev.* A **1993**, *43*, 6778−6792.
(9) Zhuang, X.; Marrucci, L.; Shen, Y. R. *Phys. Rev. Lett.* **1994**, *73*, 1513−1516.
(10) Wei, X.; Zhuang, X.; Hong, S.-C.; Goto, T.; Shen, Y. R. *Phys. Rev. Lett.* **1999**, *82*, 4256−4259.
(11) Toney, M. F.; Russel, T. P.; Logan, J. A.; Kikuchi, H.; Sands, J. M.; Kumar, S. K. *Nature* **1995**, *374*, 709−711.
(12) Samant M. G.; Stohr, J.; Brown, H. R.; Russell, T. P.; Sands, J. M.; Kumar, S. K. *Macromolecules* **1996**, *29*, 8334−8342.
(13) Seo, D.-S., Kobayashi, S., Nishikawa, M. *Appl. Phys. Lett.* **1992**, *61*, 2392−2394.
(14) Lee, K. W.; Paek, S.-H.; Lien, A.; Durning, C.; Fukuro, H. *Macronolecules* **1996**, *29*, 8894−8899.
(15) Magonov, S. N.; Reneker, D. H. *Annu. Rev. Mater. Sci.* **1997**, *27*, 175−221.
(16) Dorset, D. L.; Annis, B. K. *Macromolecules* **1996**, *29*, 2969−2973.
(17) Zhu, Y. M.; Wang, L.; Lu, Z.-H.; Wei, Y.; Chen, X. X.; Tang, J. H. *Appl. Phys. Lett.* **1994**, *65*, 49−51.
(18) Kim, Y. B.; Kim, H. S.; Choi, J. S.; Matusczyk, M.; Olin, H.; Buivydas, M.; Rudquist, P. *Mol. Cryst. Liq. Cryst.* **1995**, *262*, 89−98.
(19) Hendra, P., Jones, C., Warnes, G. *Fourier Transform Raman Spectroscopy*; Ellis Horwood: England, 1991; pp 228−259.
(20) Albrecht, M. G.; Creighton, J. A. *J. Am. Chem. Soc.* **1977**, *99*, 5215−5127.
(21) Nie, S.; Emony, S. R. *Science* **1997**, *275*, 1102−1106.
(22) Kneipp, K.; Wang, Y.; Kneipp, H.; Perelman, L. T.; Itzkan, I.; Dasari, R. R.; Feld, M. S.; *Phys. Rev. Lett.* **1997**, *78*, 1667−1670.

Scheme 2. Synthesis of the Key Diamine Monomer of Bis{ω-[4-(4-cyanophenyl)phenoxy]hexyl} 4,4′-Diamino-2,2′-biphenyldicarboxylate

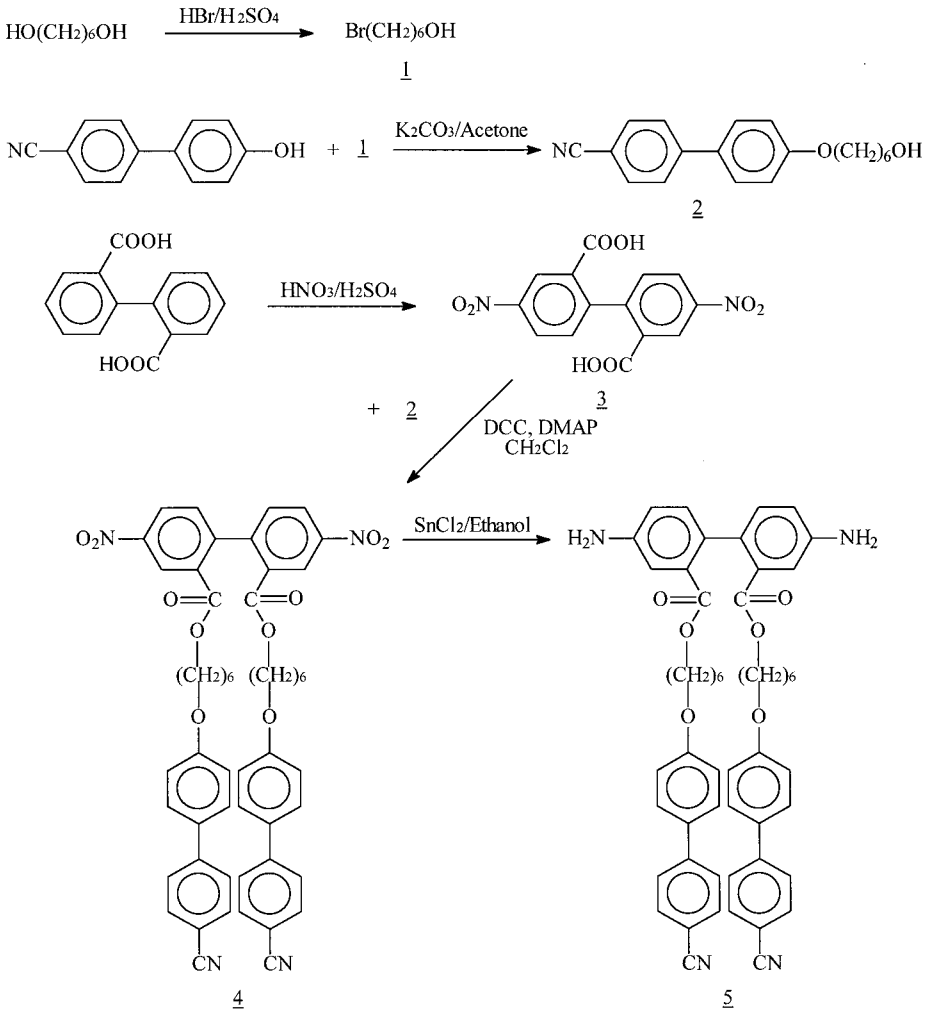

2,2′-biphenyldicarboxylate (**5**) synthesized by five steps as described in Scheme 2 (see Supporting Information).[23]

Polymerization was carried out in a one-step chemical imidiazation via polycondensation of 2,2′-bis(3,4-dicarboxyphenyl) hexafluoropropane dianhydride (6FDA) and bis{ω-[4-(4-cyanophenyl)phenoxy]-hexyl}-4,4′-diamino-2,2′-biphenyldicarboxylate (6CBBP). An equal molar ratio of the dianhydride and diamine was used in the reaction. The corresponding polymerization was conducted in a three-neck flask refluxing in a solution of *m*-cresol under a dry N_2 atmosphere with a tertiary amine catalyst (isoquinonline) at elevated temperatures for 24 h (Scheme 1). The imidiazation process was detected by Fourier transformation (FT)-IR and proton nuclear magnetic resonance spectroscopy. The intrinsic viscosity of the resulting 6FDA−6CBBP was 0.76 dL/g measured in chloroform at 30 °C. The glass transition temperature of 6FDA−6CBBP was 136 °C as measured using a Perkin-Elmer differential scanning calorimeter DSC-7 under the nitrogen atmosphere. The decomposition temperature of 2% and 5% weight loss were 326 and 358 °C, respectively, at a heating rate of 10 °C/min in dry nitrogen.

Equipment and Experiments. Rubbing was conducted on the polyimide alignment layers using a rotating drum wrapped with velvet at room temperature. The LC material ZLI-2293 (Merck Co.) was filled into the empty cells (with 10 μm spacers) in which the alignment layers were assembled into an antiparallel rubbing configuration. The pretilt angle of the alignment layers was characterized in the LC cells by the magnetic null (MN) method constructed in our laboratory. The MN method was a precise and reliable measurement for determining high pretilt angles (>10°) based on the null of the LC optical phase retardation with a continuous increase of an external magnetic field. The basic principle of this method was described in ref 24. In brief, a polarized He:Ne incident laser beam passed through a front polarizer, then a LC cell, followed by a rear polarizer (or an analyzer), and was finally detected by a position-sensitive detector. When an LC cell was rotated such that the LC molecules were oriented parallel to the external magnetic field, the light transmission was independent of the strength of the external magnetic field. The pretilt angle of alignment layers was derived from this position with a minimum optical retardation change.

Polyimide thin films for LCD alignment layers were processed by spin-coating polyimide solutions with a concentration of 2 wt % in cyclopentanone at 2000 rpm for 45 s on clean glass substrates. The films were subsequently baked at 100 °C (primary baking temperature) for 1 h and then at high temperatures between 150 and 250 °C (post-baking temperature), for an additional hour. The film thickness was controlled in the range of 50−200 nm. Thicker films (bulk samples) with thickness of 10−50 μm were also obtained by casting concentrated solutions, which were used for conventional FT-Raman measurements.

An AFM (Digital Instruments Nanoscope IIIa) was utilized in the tapping mode with phase and amplitude imaging to study topological feature changes on the polyimide surface after rubbing. The two-dimensional (2D) spectrum was converted from the height or amplitude image using the fast FT software supplied with the AFM. To observe the molecular orientation at a thin film surface on a nanometer scale, the polyethylene (PE) surface lamellar decoration (SLD) technique[25,26]

(23) Wang, S.-Y. Ph.D. Dissertation, Department of Polymer, Science, The University of Akron, Akron, OH 44325-3909.

(24) Scheffer, T. J.; Nehring, J. *J. Appl. Phys. Lett.* **1984**, *45*, 1021−1023.

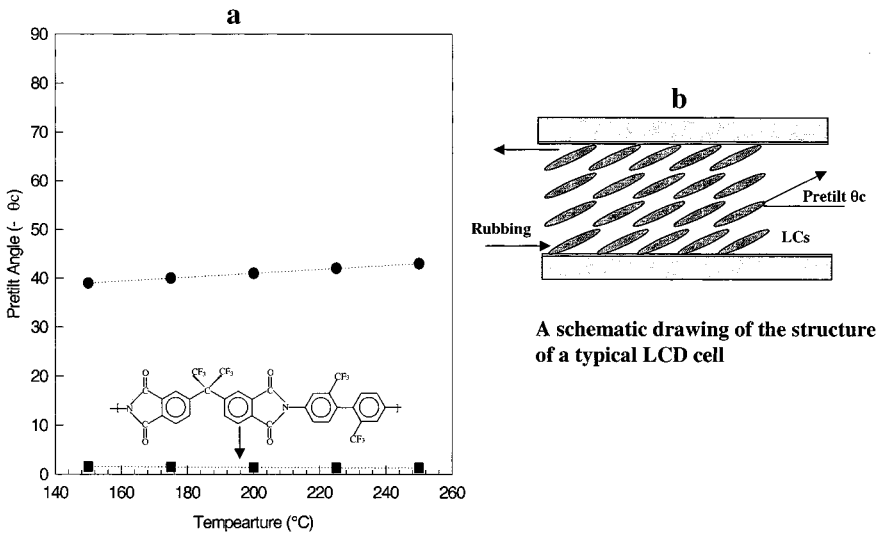

Figure 1. Pretilt angles of 6FDA−6CBBP alignment layers as a function of the post baking temperatures as well as pretilt angles of 6FDA−PFMB (the chemical structure is also included) (a); and a schematic drawing of the structure of a typical LCD cell in an antiparallel assembly (b).

was used for the first time on a rubbed film surface. In brief, a linear PE was used as the decoration material (M_n = 17 300 g/mol and polydispersity = 1.11, from Phillips Petroleum). The decoration was conducted in a vacuum evaporator. The PE was degraded, evaporated, and deposited onto the alignment-layer surface. After the PE oligomer molecules were crystallized, they were used to probe the anisotropic surfaces.

SERS-active substrates were produced using precipitation of silver colloidal aggregates through a chemical reduction of $AgNO_3$ dissolved in deionized water. An ammonia solution and dilute formaldehyde was subsequently added into the $AgNO_3$ solution to form silver colloidal aggregates on clean glass substrates. Rough silver colloids were then deposited onto the unrubbed and rubbed surfaces of the polyimide thin films.[27] The SERS measurements were conducted in a backscattering geometry on a Bruker IFS 100 FT Raman spectrometer equipped with a light source from an air-cooled Nd:YAG laser (1.064 μm) and a liquid nitrogen-cooled Ge detector. Generally, 200 scans were averaged to obtain optimum signal-to-noise ratio.

In the SHG experiment, a frequency-doubled Q-switched mode-locked Nd:YAG laser at 532 nm was used as the fundamental input beam, and the second harmonic field was detected in the reflection direction at 266 nm after proper filtering. The incidence angle was 67° with respect to the normal substrate plane on the rotation stage. The polarization dependence of SHG allowed the determination of surface molecular orientation.[8,9] The SHG process was governed by a surface nonlinear susceptibility tensor $\vec{X}^{(2)} = N\langle\vec{\alpha}^{(2)}\rangle$, where N was the surface density, $\vec{\alpha}^{(2)}$ was the hyperpolarizability tensor, and $\langle\ \rangle$ denoted the average over the orientational distribution of the molecules. From the measurement of $\vec{X}^{(2)}$ in the SHG, the approximate orientational distribution was determined assuming $\vec{\alpha}^{(2)}$ was known. In rodlike 4-cyanobiphenyls in the side chains, $\vec{\alpha}^{(2)}$ was dominated by a single element $\alpha^{(2)}_{\xi\xi\xi}$, with ξ along the long axis, and thus, the orientation distribution was directly measured from $\vec{X}^{(2)}$.[8−10]

Results and Discussion

6FDA−6CBBP Polyimide Alignment Layers Having High Pretilt Angles. Figure 1a shows a relationship between the LC pretilt angle and post-baking temperature for 6FDA−6CBBP alignment layers. When the temperature is increased from 150 to 250 °C, the pretilt angle gradually increases from 39° to 43°. The rubbed aromatic polyimide 6FDA−PFMB (the chemical structure is included in Figure 1a), which is chemically identical to the backbones of 6FDA−6CBBP, results in a low pretilt angle (1.3−1.5°), and it is independent of the post-baking temperature (also included in Figure 1a). This indicates that the pretilt angles of bulk LCs are unambiguously associated with the intrinsic polyimide chemical architectures, in which the side chains must play a vital role in generating the high pretilt angles of bulk LCs. It should be pointed out that in the past, alignment layers with high pretilt angles (>10°) have not been achieved via mechanical rubbing. It was known that the alignment layers having high pretilt angles could only be obtained via the oblique vapor deposition of inorganic SiO_x materials.

Furthermore, the pretilt angle of 6FDA−6CBBP alignment layers is uniformly oriented in a $-\theta_c$ direction, which is opposite to the conventional pretilt angle θ_c of bulk LC molecules with respect to the rubbing direction as shown in Figure 1b (a schematic drawing of a typical LC cell structure).[6−14] This unexpected observation must be associated with the specific conformation and orientation of the side chains in this polyimide at the film surface after rubbing (see below).

Surface Lamellar Decoration on Rubbed 6FDA−6CBBP Alignment Layers. To understand the molecular orientation distribution at the rubbed surface of this noncrystalline polyimide alignment layer, the SLD experiment was conducted. If the rubbing process can increase the conformation and orientation regularity at the surface, the PE oligomers may have opportunities to be aligned along the rubbing direction on the surface through short-range van der Waals interactions with 6FDA−6CBBP. As the oriented PE oligomers nucleate and crystallize at the surface, PE lamellar crystals may act as anisotropic probes to manifest the surface molecular orientation.

An amplitude image, obtained in the tapping mode AFM in Figure 2a, indeed shows a direct visualization of the orientation of PE lamellar crystals on the rubbed 6FDA−6CBBP alignment-layer surface after the SLD (on the scan area of 7.0 × 7.0 μm^2). The crystalline lamellae are in an edge-on arrangement, and the interlamellar spacing is approximately 60 nm along the rubbing direction (as indicated by the arrow in Figure 2a). Therefore, the *c*-axes of the PE lamellar crystals (the chain direction) are parallel to the short axis of the PE crystals (the rubbing direction). The long axis of the PE crystals is roughly 500 nm, which is associated with the lateral aggregation of the

(25) Wittmann, J. C.; Lotz, B. *Makromol. Rapid Commun.* **1982**, *3*, 733−738.
(26) Wittmann, J. C.; Lotz, B. *J. Polym. Sci., Polym. Phys. Ed.* **1985**, *23*, 205−226.
(27) Ge, J. J.; Xue, G.; Li, F.; McCreight, K. W.; Wang, S.-Y.; Harris, F. W.; Cheng, S. Z. D Zhuang, X.; Hong, S.-C.; Shen Y. R. *Macromol. Rapid Commun.* **1998**, *19*, 619−623.

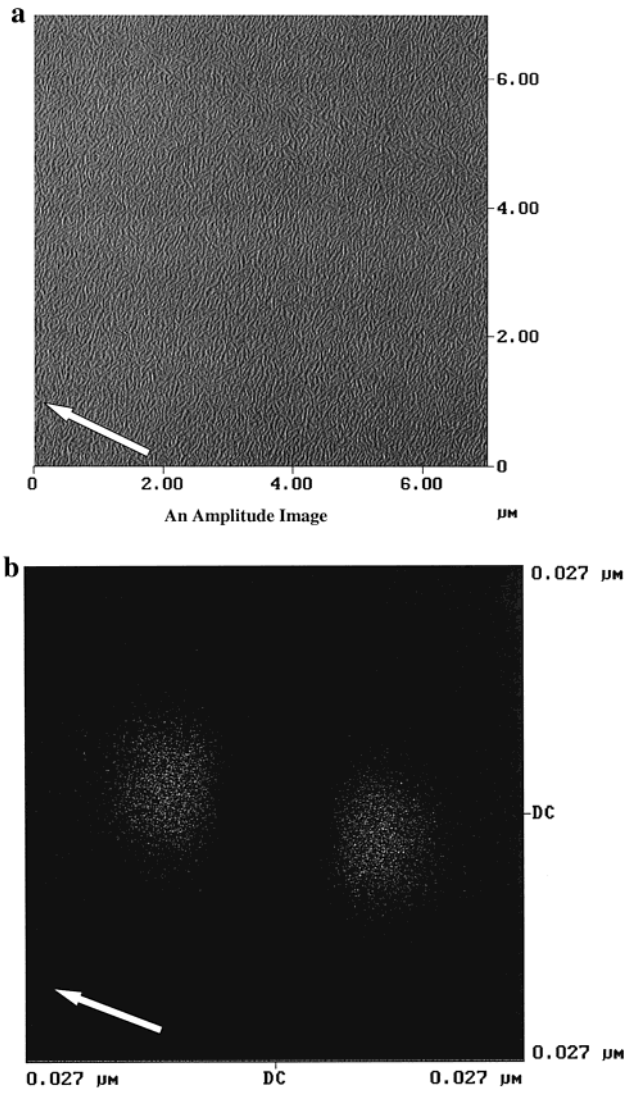

Figure 2. Tapping mode AFM morphologies of the rubbed surface of 6FDA−6CBBP after the PE lamellar crystal decoration: (a) an amplitude image at $7 \times 7\ \mu m^2$ scanning area, (b) a fast FT-2D pattern from the height image area (the rubbing direction is indicated by an arrow).

PE molecules in forming the lamellar crystals. On the other hand, the depth resolution of this SLD is less than 1 nm due to the limitation of short-range physical interactions.[25,26] This process does not require a lattice match between the PE crystal and the alignment-layer surface, since the rubbed surface is at most oriented amorphous. Therefore, this kind of SLD can be recognized as a "soft" orientation epitaxy, which only possesses a one-dimensional (1D) orientation correlation. This observation is different from the lamellar self-decoration for observing defects at the surface of LC polymers,[28] and the two-dimensional (2D) crystal epitaxy on the oriented polymer surface which requires crystal lattice matching.[29,30] It is presumable that the formation of this anisotropic surface decoration is due to the 1D uniaxial and regular conformational arrangements at the rubbed polyimide surface.

Figure 2b shows a 2D fast FT pattern from the AFM height image of the alignment-layer surface after the SLD. A spacing value of approximately 60 nm is obtained from the pair of halos

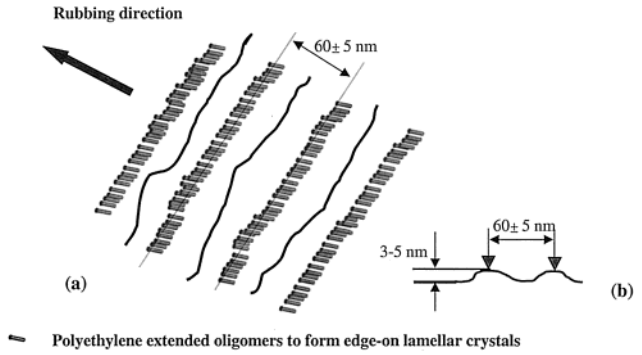

Figure 3. A schematic model of orientation epitaxy of the edge-on PE lamellar crystals on the rubbed surface of 6FDA−6CBBP (the rubbing direction is indicated by an arrow) (a); a lateral dimension of the orientation epitaxy of the PE crystals (b).

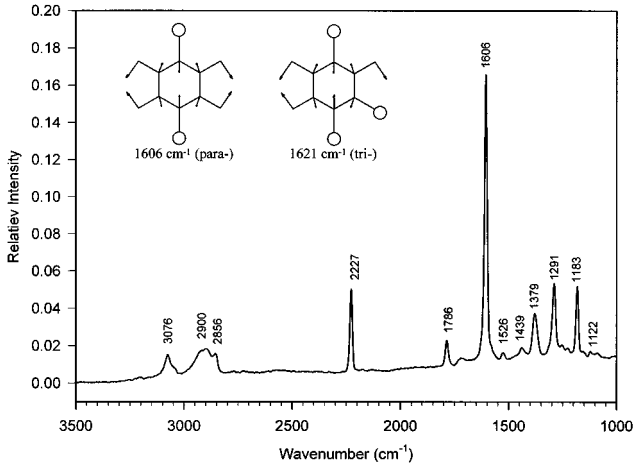

Figure 4. Normal FT-Raman spectrum of 6FDA−6 CBBP of the bulk sample (the film thickness is approximately 50 μm without rubbing).

along the rubbing direction, which is attributed to the interlamellar spacing of the edge-on PE lamellar crystals. A schematic representation of the PE lamellar crystals and their interlamellar arrangement on the rubbed polyimide surface is illustrated in Figure 3a. Each PE oligomer is represented as a rod with a length of 10−20 nm.[26] Many uniaxially oriented PE oligomers aggregate to form edge-on lamellar crystals, and the height difference of the interlamellar crystal surface is approximately 3−5 nm (see Figure 3b). Furthermore, it needs to be noted that at single-crystal surfaces of polymers, such as PE, polypropylene,[26] poly(ethylene oxide)[31] and others, the SLD observations reflect the existence of regular conformational structures on the surface, such as oriented chain folds, loops, and uniaxially extended chains, rather than dangling chains.[26] We have also used the SLD on unrubbed polyimide thin film surface; only random orientation of the PE lamellar crystals can be observed, Therefore, it is interesting to ask what kinds of the chain arrangements at the rubbed surface of 6FDA−6CBBP can lead to the observation of this uniaxial PE lamellar crystal orientation (see below).

Bulk Raman Spectra of 6FDA−6CBBP. The bulk FT-Raman spectrum recorded from a 6FDA−6CBBP thick film is shown in Figure 4. The characteristic Raman bands of the polyimide containing pendent cyanobiphenyls involve two major components: the side chains and the aromatic polyimide backbones. The characteristic bands of the imide backbones at 1786, 1379, and 1115 cm^{-1} are associated with the C═O

(28) Wood, A. B.; Thomas, E. L. *Nature* **1986**, *324*, 656−657.
(29) Wittmann, J. C.; Smith, P. *Nature* **1990**, *352*, 414−417.
(30) Damman, P.; Dosire, M.; Brunel, M.; Wittmann, J. C. *J. Am. Chem. Soc.* **1997**, *119*, 4333−4639.
(31) Chen, J.; Cheng, S. Z. D.; Wu, S. S.; Lotz, B.; Wittmann, J. C. *J. Polym. Sci., Polym. Phys. Ed.* **1995**, *33*, 1851−1855.

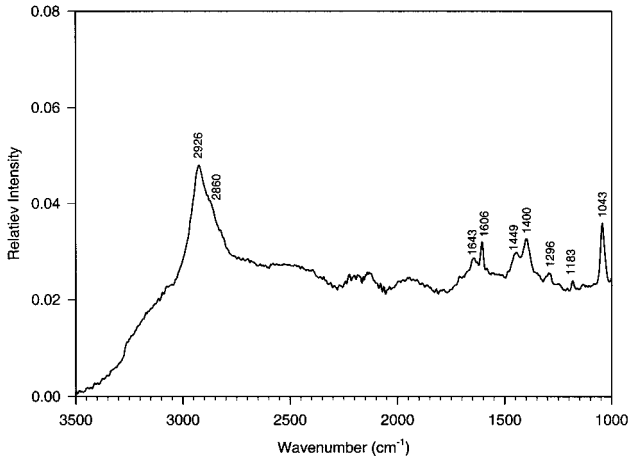

Figure 5. Surface enhanced Raman scattering spectrum of 6FDA−6CBBP from an unrubbed thin film surface contacted with a metallic layer.

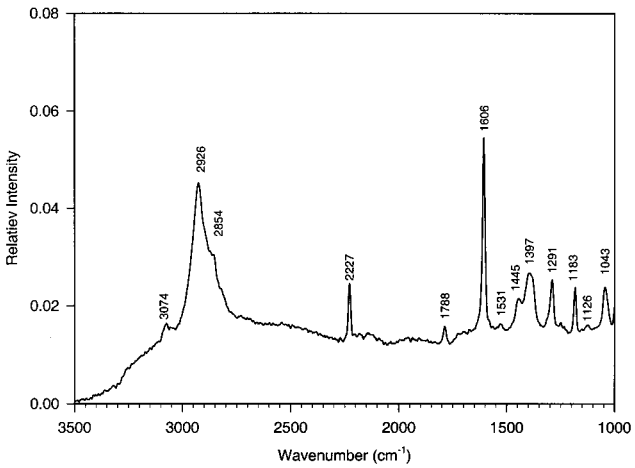

Figure 6. Surface enhanced Raman scattering spectrum of 6FDA−6CBBP from a rubbed thin film surface contacted with a metallic layer.

stretching, the axial, and transverse C−N−C stretching, respectively.[32,33] The aromatic tangential ring stretching in the backbones at 1621 cm^{-1} is partially overlapped with a stronger biphenyl tangential ring stretching at 1606 cm^{-1} of the side chains based on the model compound and peak deconvolution analyses. For the pendent cyanobiphenyls, the characteristic features arise from the aromatic C−H stretching at 3076 cm^{-1}, the aromatic-cyano stretching at 2227 cm^{-1}, the aromatic ring stretching at 1526 cm^{-1}, the C−C bridge stretching at 1290 cm^{-1} and the C−H in-plane bending ($-C_6H_4$) at 1183 cm^{-1}. In the *n*-alkyl side chains, the characteristic bands are identified at 2900 and 2856 cm^{-1} (the asymmetric and symmetric CH_2 stretching) and 1439 cm^{-1} (the CH_2 in-plane deformation), respectively.[34] When the polyimide films are thin enough (thickness < 1 μm), unenhanced FT-Raman spectroscopy is not sufficiently sensitive to collect any meaningful spectra due to a poor signal-to-noise ratio. On the other hand, unenhanced FT-Raman spectra are also not sensitive to identify subtle differences in the thick polyimide film before and after rubbing the surface, indicating that mechanically rubbing cannot substantially affect the bulk conformation and orientation changes.

Molecular Orientation at the Unrubbed 6FDA−6CBBP Thin Film Surface via SERS Measurements. After silver colloid aggregates are directly deposited onto the unrubbed 6FDA−6CBBP thin film surface, strongly enhanced Raman signals of the 6FDA−6CBBP thin films are detected as shown in Figure 5. Note that the film thickness is only around 100 nm, and therefore, the intense signals do arise from the molecules at the thin film surface adjacent to silver colloids. According to the surface selection rules of SERS for molecules adsorbed on metal surfaces, the signals of molecular vibrations with moments perpendicular to the substrate surface are intensified, while those with moments parallel to the surface are weakened.[35] This rule makes SERS surface-specific and capable of detecting the chain conformation and orientation at surfaces. In the side chains of the polyimide, the band intensities at 1606 cm^{-1} (the aromatic tangential ring stretching), 1296 cm^{-1} (the aromatic C−C bridge stretching from the $C_6H_4-C_6H_4$ components), and 1183 cm^{-1} (the C−H in-plane bending from the $-C_6H_4$ components) are weakened. The aromatic-cyano stretching vibration at 2227 cm^{-1} is absent in the SERS spectrum. As compared to the bulk FT-Raman spectrum in Figure 4, this implies that the long axis of the pendent cyanobiphenyls lies down parallel to the substrate surface. For the polyimide backbones, the C═O stretching at 1786 cm^{-1} is not detected, indicating that the imide-phenyl conjugated structure in the backbones also adopts a nearly planar conformation on the surface. In addition, the enhanced intensity of the axial C−N−C stretching in the backbones shifts to 1400 cm^{-1} away from 1379 cm^{-1} in the bulk. This shift and enhancement reflect that the presence of the side chains in the diamine moiety distorts the orientation of the axial C−N−C imide stretching, causing the vibration moment toward the direction perpendicular to the substrate surface. The medium enhancement of 1643 cm^{-1}, which can be assigned as biphenyl stretching in diamines, implies that 2,2′-substituted biphenylenes are twisted to a certain degree. Furthermore, the CH_2 asymmetric stretching at 2926 cm^{-1} (shift 26 cm^{-1} compared to the bulk spectrum) is enhanced, along with a shoulder band of the CH_2 symmetric stretching at 2860 cm^{-1}. It is probably due to the close contact of aliphatic side chains with the silver substrate.

On the basis of the SERS observations, we can qualitatively illustrate both conformations and orientations of the backbones and side chains at the surface before rubbing. The pendent cyanobiphenyls and the imide-phenylenes adopt nearly planar conformations at the surface, and the aliphatic side chains are close to the surface. This anisotropic in-plane orientation of the backbones is similar to many aromatic polyimide thin films in which the polyimide chains are oriented parallel to the substrate surface, leading to a uniaxial negative birefringence.[36,37] This study presents additional evidence that chain conformations at the surface are considerably different from those in the bulk.

Molecular Reorientation at the 6FDA−6CBBP Rubbed Thin Film Surface via SERS Measurements. Figure 6 shows the characteristic features of the SERS spectrum from the rubbed thin film surface of 6FDA−6CBBP. In this figure, the band at 1606 cm^{-1}, representing the aromatic tangential ring stretching from the cyanobiphenyls, is substantially enhanced as is the aromatic-cyano stretching band at 2227 cm^{-1}. It is deduced that

(32) Young, J. T., Tasi, W. H.; Boerio, F. J. *Macromolecules* **1992**, *25*, 887−894.
(33) Perez, M. A.; Ren, Y.; Farris, R. J.; Hsu, S. L. *Macromolecules* **1994**, *27*, 6740−6745.
(34) Hallmark, V. M.; Zimba, C. G.; Sooriyakuamaran, Miller, R. D.; Rabolt, J. F. *Macromolecules* **1990**, *23*, 2346−2350.
(35) Moskovits, M. *J. Chem. Phys*. **1982**, *77*, 4408−4416.
(36) Cheng, S. Z. D.; Arnold, F. E., Jr.; Zhang, A.; Hsu, S. L.; Harris, F. W. *Macromolecules* **1991**, 24, 5856−5862.
(37) Li, F.-M.; Kim, K.-H.; Savitski, E. P.; Chen, J.-C.; Yoon, Y.; Harris, F. W.; Cheng, S. Z. D. In *Photonic and Optoelectronic Polymers*; ACS Symposium Series; American Chemical Society: Washington, DC, 1997; Vol. 672, pp 1−14, 1997.

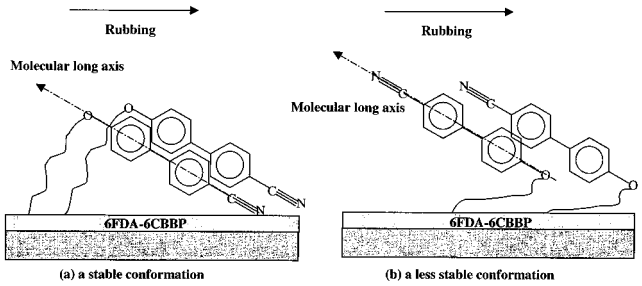

Figure 7. A schematic model of the molecular orientation of pendent cyanobiphenyls on the rubbed side chain polyimide surface of 6FDA−6CBBP: (a) a stable conformation and (b) a less stable conformation. Both of the long axis orientation of the tilt cyanobiphenyls is opposite to the rubbing direction.

the cyanobiphenyls in the side chains adopt a tilted conformation with respect to the surface substrate after rubbing, significantly different from the nearly planar conformation before rubbing (see Figure 5). Note that the long axis of cyanobiphenyls is tilted approximately 41 ± 2° from the layer surface, in the direction opposite that of the rubbing, as determined by the MN method via LC orientation epitaxy at the surface. Further supporting evidence comes from the drastic increase in intensities of the bands at 1291 cm^{-1} (the aromatic C−C bridge stretching of the $C_6H_4-C_6H_4$ components) and 1183 cm^{-1} (the CH in-plane bending of the $-C_6H_4$ components). The axial C−N−C stretching band at 1397 cm^{-1} in the linkage between the dianhydride and diamaine is also enhanced and shifts 18 cm^{-1} from 1379 cm^{-1} in the bulk (Figure 4). This observation confirms the existence of the nonplanar conformation in the linkage. The appearance of the carbonyl band at 1788 cm^{-1} suggests that the rubbing process also causes the rigid imidephenyl structure or 2,2′-substituted biphenylene of the backbones to slightly tilt from the substrate, leading to a small deviation of the polyimide backbones from the planar arrangement. A new, small band at 1126 cm^{-1} of the transverse C−N−C stretching mode appears and shifts from the 1122 cm^{-1} band in the bulk. This may imply an increase in ordering of the imide ring packing at the surface after rubbing.[33] In the aliphatic side chains, the CH_2 in-plane deformation shifts to 1445 cm^{-1} from the original surface band at 1449 cm^{-1}, while the CH_2 symmetric stretching shifts toward 2854 cm^{-1} on the surface from the original 2860 cm^{-1}. Note that these frequency shifts are probably associated with changes in aliphatic chain conformations interacting with the silver substrate. Since the aliphatic side chains connect the pendent cyanobiphenyls with the backbones, these chains must act as linkages to support the cyanobiphenyl to form a regular and stable conformation on the rubbed surface (see below).

The significantly enhanced signals of the cyanobiphenyls in the side chains indicate that the cyanobiphenyl units must play a critical role in generating the pretilt angle and the tilting direction on the surface. Considering that the orientation direction of LCs is opposite to the rubbing direction, the tilted cyanobiphenyl conformation at the surface must be self-assembled into one of two possible arrangements as shown in Figure 7 a and b. In the case of Figure 7a, the cyanobiphenyls are tilted from the surface with the cyano groups pointing down toward the layer surface, which is similar to the chain folding at polymer crystal-basal surfaces. In the other case of Figure 7b, the cyanobiphenyls are tilted from the surface with the cyano groups pointing up with respect to the surface. This is close to the case of dangling chain ends on the crystal surface. Since the cyanobiphenyls of the side chains can form attractive interactions with the backbones at the layer surface, the fold-like bent conformation in Figure 7a should be more stable and favorable. Furthermore, the dangling chain ends on the surface do not generate a stable high pretilt angle with a uniaxial orientation, and no clear regular PE decoration image can be probed on the surface.[26] Therefore, the SDL results also support the existence of the unique and stable fold-like bent conformation, which allows us to fabricate uniform LC cells. However, this conformational arrangement has to be determined by examining the cyanobiphenyl orientation at the alignment-layer surface.

Cyanobiphenyl Orientation at the Rubbed Thin Film Surface via SHG Measurements. The surface SHG results further demonstrate that, after rubbing the 6FDA−6CBBP thin film, those pendent cyanobiphenyls in the side chains possess a significantly anisotropic azimuthal distribution at the alignment-layer surface along the $-\theta_c$ direction. Since the cyanobiphenyls are chromophores, which have a hyper-polarizability tensor $\vec{\alpha}^{(2)}$ dominated by a single element $\alpha^{(2)}_{\xi\xi\xi}$, its orientation can be deduced from the nonlinear susceptibility tensor $\vec{X}^{(2)}$ determined by measuring an azimuthal variation of SHG with four input/output polarization combinations,[8−10] as shown in Figure 8. The insert in this figure provides the definition of the polar orientation angle θ, which utilizes the angle between the cyanobiphenyl long axis and the *z*-axis. The azimuthal angle (ϕ) is constructed between the projection of this long axis and the *x*-axis in the *xy* plane. These two parameters determine the average direction of the cyanobiphenyl long axis, and thus, the pretilt angle orientation at the rubbed surface in three-dimensional real space. For the cyanobiphenyl long axis at the 6FDA−6CBBP alignment-layer surface having an orientation distribution of $f(\theta,\phi)$, the surface nonlinear susceptibility can be obtained as a function of $f(\theta,\phi)$. Since the cyanobiphenyl long axis at the surface possesses C_{1v} symmetry, five parameters of θ_0, σ, d_1, d_2, and d_3 can be deduced from the nonlinear susceptibility measurements based on the approximate distribution function equation of

$$f(\theta,\phi) = A\exp[-(\theta-\theta_0)^2/2\sigma^2](1 + d_1\cos\phi + d_2\cos 2\phi + d_3\cos 3\phi)$$

Note that for the isotropic samples the SHG signals with an *s*-polarized output are forbidden due to inversion symmetry. However, the SHG intensity from the rubbed surface is considerably anisotropic, indicating that the rubbing process induces a significant rearrangement of the cyanobiphenyl orientation. Detailed data fitting (the solid lines in Figure 8 a−d) allows us to determine six independent nonvanishing elements of $\vec{X}^{(2)}$. Their corresponding values

$$\chi^{(2)}_{xxx}:\ \chi^{(2)}_{xyx}:\ \chi^{(2)}_{xzz}:\ \chi^{(2)}_{zxx}:\ \chi^{(2)}_{zyy}:\ \chi^{(2)}_{zzz} = 1:\ 0.22:\ 0.031:\ -0.12:\ -0.072:\ -0.041$$

and their errors are ±5, ±20, ±10, ±20, and ±25%, respectively. Even though $\vec{X}^{(2)}$ for 6FDA−6CBBP originates mainly from the cyanobiphenyls in the side chains, it has also been found in a polyimide of 6FDA−PFMB (see the chemical structure in Figure 1a), which has identical backbones but no side chains, the field discontinuity at the surface along *z* contributes a value of $\chi^{(2)}_{zzz}$ (6FDA−PFMB) = 0.012.[38] This value is big enough when compared to the value of $\chi^{(2)}_{zzz} = -0.041$ at the surface of 6FDA−6CBBP, which attributes to both contributions

(38) Hong, S.-C.; Oh, M.; Zhuang, X.; Shen, Y. R.; Ge, J. J.; Harris, F. W.; Cheng, S. Z. D. *Phys. Rev. E* **2001.** In press.

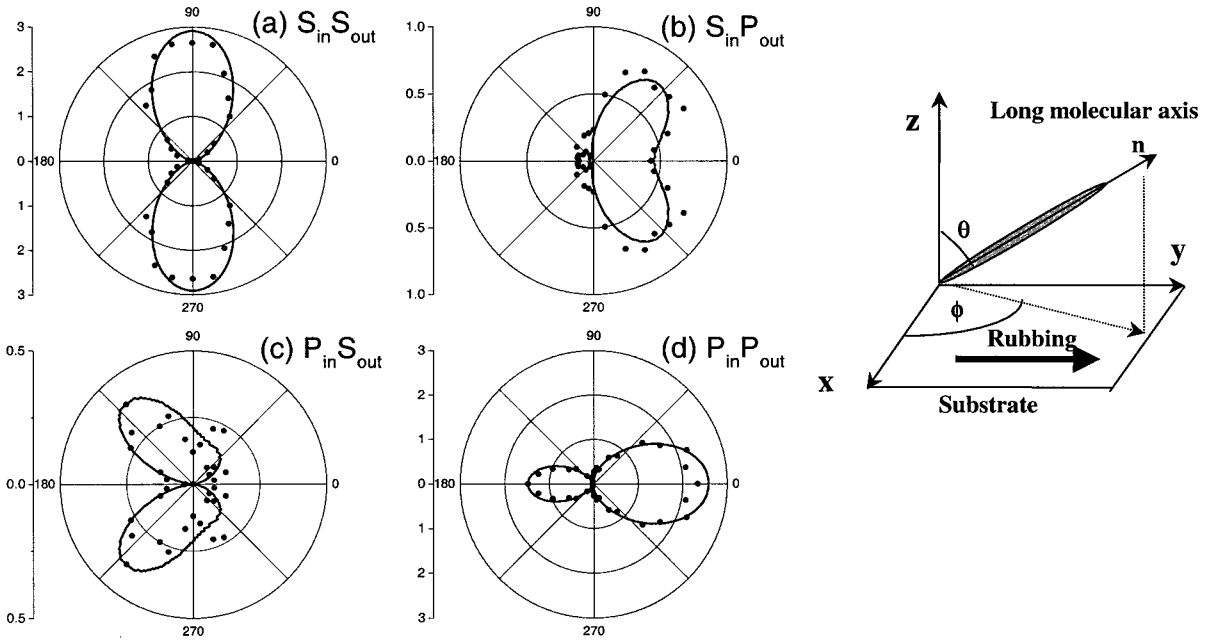

Figure 8. Anisotropic optical SHG results from 6FDA−6CBBP rubbed thin layer surfaces. They are *s*-input and *s*-output (a); *s*-input and *p*-output (b); *p*-input and *s*-output (c); and *p*-input and *p*-output (d). Circles are experimental data and lines which are fitted using the equation in the text. The insert is the geometry definition of the rubbed surface.

of the backbones and cyanobiphenyls in the side chains. Therefore, the difference between these two values is the true contribution of the cyanobiphenyls at the surface of the 6FDA−6CBBP. Contributions of the field discontinuity of the other elements of $\vec{\vec{X}}^{(2)}$ (except for $\chi^{(2)}_{zzz}$) are much weaker and can be considered negligible. The deduced parameters can thus be calculated as: $\theta_o = 84.6$, $\sigma = 12.0$, $d_1 = -1.03$, $d_2 = 0.50$, and $d_3 = -0.29$. Note that the d_1 value is negative, implying that that cyanobiphenyls in the side chains are aligned opposite to the rubbing direction.

However, the SHG intensity measurements cannot directly distinguish those two different possible cyanobiphenyl orientations, as shown in Figure 7 a and b. To search for the definitive answer, an SHG phase measurement is introduced. The cyanobiphenyls in the side chains with opposite orientations (in Figure 7 a and b) should cause a 180°-phase difference in the element $\chi^{(2)}_{zzz}$. On the other hand, a well-known example of cyanobiphenyl groups in 5CB monolayer aligned on a commercially available polyimide alignment-layer surface (P6 which does not contain side chains) shows that the cyanobiphenyls point down toward the polyimide-layer surface having a pretilt angle of θ_c as shown in Figure 9a.[38] Since the SHG phase measurements are critically associated with the polar vector along the cyanobiphenyl long axis, the arrangements between Figures 7a and 9a should also lead to a 180°-phase difference in the element $\chi^{(2)}_{zzz}$. However, if the cyanobiphenyls are arranged as shown in Figure 7b, there should be no phase difference in $\chi^{(2)}_{zzz}$ compared with that in Figure 9a. As seen from the measured interference patterns for both of the cases in Figure 9 b and c, the measured SHG $X^{(2)}_{zzz}$ phase of the cyanobiphenyls in 6FDA−6CBBP (in Figure 9b) is opposite to that of 5CB monolayer absorbed on the polyimide alignment layer P6 (in Figure 9c). Therefore, it can be concluded that the orientation of the cyanobiphenyls in the side chains of 6FDA−6CBBP is as described in Figure 7a. This leads to a fold-like bent conformational structure. The molecular mechanism of observing a negative pretilt angle in the LC bulk alignment is thus the specific orientation of the pendent cyanobiphenyls in the side chains at the rubbed surface. It is also expected that the high pretilt angle is controllable by varying the number of methylene units and chemical linkages of the side chains in this series of polyimides.

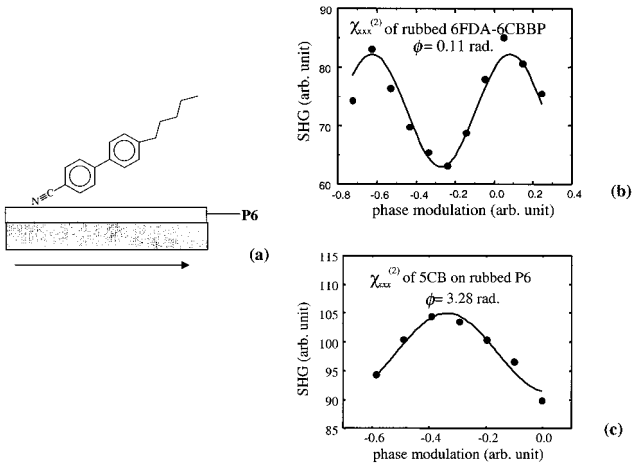

Figure 9. Schematics describing the orientation of 5CB LC monolayer absorbed on a commercial polyimide (P6) alignment-layer surface. The cyano groups point down toward the layer surface and the pretilt angle is θ_c with respect to the rubbing direction. The arrow represents the rubbing direction (a). The experimental data points and the fitting curves in (b) and (c) represent the results of SHG phase measurements of $\chi^{(2)}_{xxx}$ on the surface of the rubbed 6FDA−6CBBP and 5CB monolayer on the surface of the rubbed P6 alignment layer.

Conclusions

The aromatic polyimide 6FDA−6CBBP which contains pendent cyanobiphenyls in the side chains has been designed and synthesized for achieving high pretilt angle alignment layers. After mechanical rubbing at room temperature, high pretilt angles are aligned in the $-\theta_c$ direction opposite to the rubbing direction as detected by both MN and SHG experiments. In the SLD experiments, when PE oligomers are nucleated and crystallized at the rubbed alignment surface, edge-on PE lamellar

crystals directly probe the anisotropic molecular orientation at the surface observed in AFM. The PE chains in the crystals are oriented parallel to the rubbing direction. A 2D fast FT pattern from the AFM height image verifies that the anisotroptic and preferential orientation of the PE crystals is induced on the rubbed polymer surface. Nearly planar molecular conformations in both the backbones and the pendent mesogens (in-plane orientation) at the original polyimide surface can be identified using SERS. After rubbing, the uniform reorientation and rearrangement of the pendent cyanobiphenyl conformations at the rubbed surface are the major cause of generating the high pretilt angles opposite to the rubbing direction. The alignment mechanism of this rubbed 6FDA−6CBBP can be further deduced to attribute to the specific orientation of the cyanobiphenyls in the side chains. The long axis of the cyanobiphenyls are anisotropically tilted from the surface by rubbing, and the cyano groups prefer pointing down toward the polyimide-layer surface to form a stable, fold-like bent conformation.

Acknowledgment. This work was supported by the NSF Science and Technology Center of Advanced Liquid Crystalline Optical Materials (ALCOM, DMR-91-57738), Nitto Denko Corporation, and NSF DMR-96-17030.

Supporting Information Available: Detailed experimental routes for the syntheses of monomers (**1**), (**2**), (**3**), (**4**) and (**5**) in Scheme 1 (PDF). This material is available free of charge via the Internet at http://pubs.acs.org.

JA0042682